

Effect of terminal N-substitution in 2-oxo-1,2-dihydroquinoline-3-carbaldehyde thiosemicarbazones on the mode of coordination, structure, interaction with protein, radical scavenging and cytotoxic activity of copper(II) complexes†Duraiamy Senthil Raja,^a Ganesan Paramaguru,^b Nattamai S. P. Bhuvanesh,^c Joseph H. Reibenspies,^c Rajalingam Renganathan^b and Karuppannan Natarajan^{*a}

Received 29th November 2010, Accepted 18th February 2011

DOI: 10.1039/c0dt01657h

Four 2-oxo-1,2-dihydroquinoline-3-carbaldehyde N-substituted thiosemicarbazone ligands (H₂-OQtsc-R, where R = H, Me, Et or Ph) and their corresponding new copper(II) complexes [CuCl₂(H₂-OQtsc-H)·2H₂O (**1**), [CuCl₂(H₂-OQtsc-Me)·2H₂O (**2**), [CuCl₂(H₂-OQtsc-Et)(CH₃OH)]Cl (**3**) and [CuCl(H-OQtsc-Ph)]·CH₃OH (**4**) have been synthesized in order to correlate the effect of terminal N-substitution on coordination behaviour, structure and biological activity. Single crystal X-ray diffraction studies revealed that the complexes **1**, **2** and **3** have square pyramidal geometry around the central metal ion. In the complexes **1** and **2**, the copper ion is coordinated by the ligand with ONS donor atoms, one chloride ion in apical position and the other chloride in the basal plane. Complex **3** consists of [CuCl₂(H₂-OQtsc-Et)(CH₃OH)]⁺ cation and a chloride as counter ion. The copper ion is coordinated by the ligand with ONS donor atoms and by one chloride ion in the basal plane. One methanol molecule is bonded through its neutral oxygen in the apical position. Complex **4** is square planar with the ligand coordinating through uni-negative tridentate ONS⁻ and by one chloride ion in the basal plane. The binding of complexes with lysozyme protein was carried out by fluorescence spectroscopy. Investigations of antioxidation properties showed that all the copper(II) complexes have strong radical scavenging properties. The cytotoxicity of the complexes **3** and **4** against NIH 3T3 and HeLa cell lines showed that synergy between the metal and ligands results in a significant enhancement in the cell death with IC₅₀ of ~10–40 μM. A size dependence of substitution at terminal N in the thiosemicarbazones on the biological activities of the complexes has been observed.

Introduction

Thiosemicarbazones form an important class of compounds because of their promising pharmacological properties, such as trypanocidal activity,¹ antitubercular activity,² and antitumor activities.^{3,4} Some thiosemicarbazones have shown to increase

their biological activity by their ability to form chelates with specific metal ions.⁵ Among the transition metal ions, Cu(II) is a biologically essential ion whose positive redox potential permits involvement in biological electron transfer reactions.⁶ Copper(II) complexes of thiosemicarbazones have engrossed considerable interest because of their variable bonding properties, structural diversity, and pharmacological properties.^{7–9}

In general, drug interactions at the protein binding level will exert significant effect on the apparent distribution volume and the elimination rate of drugs. Therefore, it is necessary to study the interactions between drugs and proteins. Lysozyme is an enzyme which has six tryptophan and three tyrosine residues in its structure.¹⁰ The important function of lysozyme is the transportation of the drugs to the required places and the effectiveness of drugs depends on their binding ability with lysozyme. In this connection, the interactions between proteins and small molecules, such as metal ions, nonmetal ions, dyes, complexes and numerous pharmaceuticals have been extensively studied.^{11–17} Therefore, a study of the interaction of biologically active metal complexes with lysozyme is important to derive

^aDepartment of Chemistry, Bharathiar University, Coimbatore, 641046, India. E-mail: k_natraj6@yahoo.com; Fax: +91 422 2422387; Tel: +91 422 2428319

^bSchool of Chemistry, Bharathidasan University, Tiruchirappalli, 620024, India

^cDepartment of Chemistry, Texas A&M University, College Station, TX, 77843, U.S.A

† Electronic supplementary information (ESI) available: Crystal packing diagram of the unit cell showing hydrogen bonding of **1**, **2**, **3** and **4** (Figures S1–S4), Emission spectra of binding of **1**, **2**, **3** and **4** with Protein (Figures S5–S7), Absorption spectra of binding of **1**, **2** and **3** with Protein (Figures S8–S10), Synchronous spectra (Δλ = 15 nm) of binding of **1**, **2**, **3** and **4** with Protein (Figures S11–S14), Synchronous spectra (Δλ = 60 nm) of binding of **1**, **2** and **3** with Protein (Figures S15–S17). CCDC reference numbers 763001, 763002, 772056 and 772085. For ESI and crystallographic data in CIF or other electronic format see DOI: 10.1039/c0dt01657h

useful information regarding the therapeutic effectiveness of metal complexes. Moreover, recent reports have also suggested that many transition metal complexes have exhibited interesting antioxidant activities.^{18,19}

In the case of pharmaceuticals, in addition to thiosemicarbazones, nitrogen heterocycles have also exhibited remarkable biological activities.^{20–22} In particular, some derivatives of 2-oxoquinoline have shown biological activities such as antioxidation,²³ antiproliferation,²⁴ anti-inflammation,²⁵ and anticancer.²⁶ While extensive work has been carried out with thiosemicarbazone complexes, only a little attention has been paid to the corresponding complexes derived from 2-oxo-1,2-dihydroquinoline-3-carbaldehyde.²⁷

Though the effect of substitution on terminal N of thiosemicarbazones on the biological properties of the complexes formed and on the coordination behaviour of thiosemicarbazones have been reported,^{28–34} there is no systematic investigation on the effect of such substitution in thiosemicarbazones is known.

Here, we report synthesis, characterization, crystal structures and biological activities of four copper(II) complexes of 2-oxo-1,2-dihydroquinoline-3-carbaldehyde N-substituted thiosemicarbazones. The synthetic routes of the ligands and the complexes are shown in Scheme 1.

Experimental Section

General

All the starting materials and reagent grade solvents were purchased from standard commercial sources and used without further purification. 2-oxo-1,2-dihydroquinoline-3-carbaldehyde³⁵ and H₂-OQtsc-H²⁷ were prepared as reported; the latter with some modifications as described below. Elemental analyses (C, H, N, S) were performed on Vario EL III Elementar analyzer instrument. IR spectra (4000–400 cm⁻¹) were recorded on a Nicolet Avatar Model FT-IR spectrophotometer. ¹H NMR spectra was recorded on Bruker AMX 500 at 500 MHz using tetramethylsilane as an internal standard. Melting points were determined with a Lab India instrument. Electronic absorption spectra were recorded by Jasco V-630 spectrophotometer. Emission spectra were measured

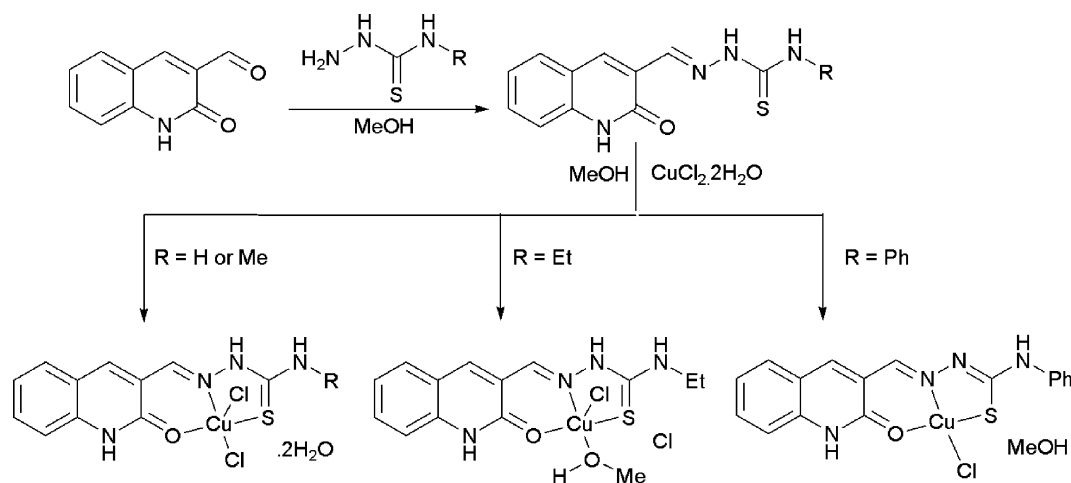
by Jasco FP 6600 spectrofluorometer. Magnetic susceptibilities at room temperature were measured on a Faraday balance using mercury(II) tetrathiocyanatocobalt(II) as calibrant.

Preparation of the ligands

2-oxo-1,2-dihydroquinoline-3-carbaldehyde thiosemicarbazone (H₂-OQtsc-H). Thiosemicarbazide (911 mg, 0.01 mol) dissolved in warm methanol (50 ml) was added to a methanol solution (50 ml) containing 2-oxo-1,2-dihydroquinoline-3-carbaldehyde (1.73 g, 0.01 mol). The mixture was refluxed for an hour during which period a yellow precipitate was formed. The reaction mixture was then cooled to room temperature and the solid compound was filtered. It was then washed with methanol and dried under vacuum. Yield = 92%. Mp: 296 °C. Anal. Calcd for C₁₁H₁₀N₄OS: C, 53.64; H, 4.09; N, 22.75; S, 13.02%. Found: C, 53.42; H, 4.11; N, 22.71; S, 13.12%. IR (KBr disks, cm⁻¹): 3154(ms) ν(NH); 1644(s) ν(C=O); 1582(s) ν(C=N) + ν(C=C); 1461(ms) ν(CSN); 871(m) ν(C=S). UV-visible (solvent MeOH, nm): 382 (n→π* & π→π*). ¹H NMR (DMSO-D₆, ppm): 11.98 (s, 1H, N(3)H); 11.62 (s, 1H, N(1)H); 8.75 (s, 1H, C(1)H); 8.28 (s, 2H, N(4)H₂); 8.27 (s, 1H, C(6)H); 7.62 (d, 1H, C(10)H); 7.53 (t, 1H, C(9)H); 7.32 (d, 1H, C(7)H); 7.22 (t, 1H, C(8)H).

2-oxo-1,2-dihydroquinoline-3-carbaldehyde N-methylthiosemicarbazone (H₂-OQtsc-Me). It was prepared using the same procedure as described for H₂-OQtsc-H with 4-methyl-3-thiosemicarbazide (1.05 g, 0.01 mol) and 2-oxo-1,2-dihydroquinoline-3-carbaldehyde (1.73 g, 0.01 mol). A yellow product was obtained. Yield = 89%. Mp: 299 °C. Anal. Calcd for C₁₂H₁₂N₄OS: C, 55.37; H, 4.65; N, 21.52; S, 12.32%. Found: C, 55.36; H, 4.63; N, 21.53; S, 12.35%. IR (KBr disks, cm⁻¹): 3156(ms) ν(NH); 1648(s) ν(C=O); 1554(s) ν(C=N) + ν(C=C); 1430(ms) ν(CSN); 877(m) ν(C=S). UV-visible (solvent MeOH, nm): 383 (n→π* & π→π*). ¹H NMR (DMSO-D₆, ppm): 12.03 (s, 1H, N(3)H); 11.71 (s, 1H, N(1)H); 8.67 (s, 1H, C(1)H); 8.60 (s, 2H, N(4)H); 8.27 (s, 1H, C(6)H); 7.67 (d, 1H, C(10)H); 7.52 (t, 1H, C(9)H); 7.31 (d, 1H, C(7)H); 7.22 (t, 1H, C(8)H); 3.04 (s, 3H, C(12)H).

2-oxo-1,2-dihydroquinoline-3-carbaldehyde N-ethylthiosemicarbazone (H₂-OQtsc-Et). It was prepared using the same



Scheme 1 Preparation routes of the ligands and the copper complexes.

procedure as described for H₂-OQtsc-H with 4-ethyl-3-thiosemicarbazide (1.19 g, 0.01 mol) and 2-oxo-1,2-dihydroquinoline-3-carbaldehyde (1.73 g, 0.01 mol). An yellow compound was obtained. Yield = 90%. Mp: 303 °C. Anal. Calcd for C₁₃H₁₄N₄O₂S: C, 56.91; H, 5.14; N, 20.42; S, 11.69%. Found: C, 56.91; H, 5.11; N, 20.43; S, 11.71%. IR (KBr disks, cm⁻¹): 3140(ms) v(NH); 1649(s) v(C=O); 1531(s) v(C=N) + v(C=C); 1429(ms) v(CSN); 879(m) v(C=S). UV-visible (solvent MeOH, nm): 384 (n→π* & π→π*). ¹H NMR (DMSO-D₆, ppm): 12.03 (s, 1H, N(3)H); 11.65 (s, 1H, N(1)H); 8.65 (s, 1H, C(1)H); 8.62 (s, 2H, N(4)H); 8.27 (s, 1H, C(6)H); 7.67 (d, 1H, C(10)H); 7.51 (t, 1H, C(9)H); 7.31 (d, 1H, C(7)H); 7.22 (t, 1H, C(8)H); 3.61 (q, 2H, C(12)H); 1.17 (t, 3H, C(13)H).

2-oxo-1,2-dihydroquinoline-3-carbaldehyde N-phenylthiosemicarbazone (H₂-OQtsc-Ph). It was prepared using the same procedure as described for H₂-OQtsc-H with 4-phenyl-3-thiosemicarbazide (1.67 g, 0.01 mol) and 2-oxo-1,2-dihydroquinoline-3-carbaldehyde (1.73 g, 0.01 mol). An yellow compound was obtained. Yield = 94%. Mp: 316 °C. Anal. Calcd for C₁₇H₁₄N₄O₂S: C, 63.33; H, 4.38; N, 17.38; S, 9.95%. Found: C, 63.39; H, 4.35; N, 17.37; S, 9.95%. IR (KBr disks, cm⁻¹): 3304(ms) v(NH); 1654(s) v(C=O); 1534(s) v(C=N) + v(C=C); 1442(ms) v(CSN); 891(m) v(C=S). UV-visible (solvent MeOH, nm): 387 (n→π* & π→π*). ¹H NMR (DMSO-D₆, ppm): 12.05 (s, 1H, N(3)H); 11.95 (s, 1H, N(2)H); 10.17 (s, 1H, N(4)H); 8.87 (s, 1H, C(1)H); 8.39 (s, 1H, C(6)H); 7.24–7.68 (m, 9H, aromatic).

Synthesis of complexes

[CuCl₂(H₂-OQtsc-H)]·2H₂O (1). A warm methanolic solution (20 ml) containing H₂-OQtsc-H (123 mg, 0.5 mmol) was added to a methanolic solution (10 ml) of CuCl₂·2H₂O (85 mg, 0.5 mmol). The resulting greenish solution was refluxed for an hour. Green crystals were obtained on slow evaporation. They were filtered off, washed with cold methanol, and dried under vacuum. Yield = 86%. Mp: 327 °C. Anal. Calcd for C₁₁H₁₄Cl₂Cu N₄O₃S: C, 31.70; H, 3.39; N, 13.44; S, 7.96%. Found: C, 31.71; H, 3.43; N, 13.47; S, 7.95%. IR (KBr disks, cm⁻¹): 3152(ms) v(NH); 1640(s) v(C=O); 1604(s) v(C=N) + v(C=C); 1543 (ms) v(CSN); 862(m) v(C=S). UV-visible (solvent MeOH, nm): 297 (Intra-Ligand Charge Transfer (ILCT)); 399 (Metal to Ligand Charge Transfer (MLCT)). μ_{eff} (300 K): 1.67 μ_B.

[CuCl₂(H₂-OQtsc-Me)]·2H₂O (2). It was prepared using the same procedure as described for **1** with H₂-OQtsc-Me (130 mg (0.5 mmol) and CuCl₂·2H₂O (85 mg, 0.5 mmol). Green crystals were obtained. Yield = 85%. Mp: 331 °C. Anal. Calcd for C₁₂H₁₆Cl₂Cu N₄O₃S: C, 33.46; H, 3.74; N, 13.01; S, 7.44%. Found: C, 33.47; H, 3.73; N, 12.98; S, 7.45%. IR (KBr disks, cm⁻¹): 3151(ms) v(NH); 1637(s) v(C=O); 1590(s) v(C=N) + v(C=C); 1547 (ms) v(CSN); 868(m) v(C=S). UV-visible (solvent MeOH, nm): 298 (ILCT); 402 (MLCT). μ_{eff} (300 K): 1.69 μ_B.

[CuCl₂(H₂-OQtsc-Et)(CH₃OH)]Cl (3). It was prepared using the same procedure as described for **1** with H₂-OQtsc-Et (137 mg (0.5 mmol) and CuCl₂·2H₂O (85 mg, 0.5 mmol). Green crystals were obtained. Yield = 89%. Mp: 335 °C. Anal. Calcd for C₁₄H₁₈Cl₂Cu N₄O₂S: C, 38.14; H, 4.12; N, 12.71; S, 7.27%. Found: C, 38.13; H, 4.08; N, 12.62; S, 7.25%. IR (KBr disks, cm⁻¹): 3213(mw) v(OH) 3121(ms) v(NH); 1642(s) v(C=O); 1589(s) v(C=N) +

v(C=C); 1539 (ms) v(CSN); 869(m) v(C=S). UV-visible (solvent MeOH, nm): 298 (ILCT); 403 (MLCT). μ_{eff} (300 K): 1.72 μ_B.

[CuCl(H-OQtsc-Ph)]·CH₃OH (4). It was prepared using the same procedure as described for **1** with H₂-OQtsc-Ph (161 mg (0.5 mmol) and CuCl₂·2H₂O (85 mg, 0.5 mmol). Green crystals were obtained. Yield = 93%. Mp: 353 °C. Anal. Calcd for C₁₈H₁₇ClCu N₄O₂S: C, 47.79; H, 3.79; N, 12.38; S, 7.09%. Found: C, 47.77; H, 3.78; N, 12.32; S, 7.05%. IR (KBr disks, cm⁻¹): 3314(mw) v(OH) 3331(ms) v(NH); 1644(s) v(C=O); 1547(s) v(C=N) + v(C=C); 1487(ms) v(CSN); 812(m) v(C-S). UV-visible (solvent MeOH, nm): 299 (ILCT); 412 (MLCT). μ_{eff} (300 K): 1.77 μ_B.

Single-crystal X-ray diffraction studies

Single-crystal X-ray diffraction data of the complexes **2**, **3** and **4** were collected on a Bruker three-circle platform diffractometer equipped with a SMART 1000 CCD detector. Data for complex **1** was collected using the GADDS instrument with a Cu source and a multiwire detector. Integrated intensity information for each reflection was obtained by reduction of the data frames with the program SAINTplus³⁶ for **1** and APEX2³⁷ for the remaining **2**, **3** and **4**. The integration method employed a three dimensional profiling algorithm and all data were corrected for Lorentz and polarization factors, as well as for crystal decay effects. All non-hydrogen atoms were refined with anisotropic thermal parameters. The hydrogen atoms bound to carbon were placed in idealized positions and refined using riding model. Hydrogen atoms attached to N and O were located from the Fourier difference maps and was set riding on the respective parent atom. All the structures were refined (weighted least squares refinement on *F*²) to convergence.³⁸ Mercury software was employed for the structure plots.³⁹ Though two water molecules are present in **1** and **2**, the occupancy factor of one of the water molecules was found to be 0.9 for **1** and 0.5 for **2**. A crystal with two (non-merohedral) twin components was used for data collection and the final least squares refinement was carried out with reflections from both the components for **2**. Relevant data concerning data collection and details of structure refinement are summarized in Table 1.

Protein binding studies

The excitation wavelength of lysozyme at 280 nm and the emission at 347 nm were monitored for the protein binding studies. The excitation and emission slit widths and scan rates were maintained constant for all the experiments. Samples were carefully degassed using pure nitrogen gas for 15 min. Quartz cells (4 × 1 × 1 cm) with high vacuum Teflon stopcocks were used for degassing. Stock solution of lysozyme was prepared in 50 mM phosphate buffer (pH = 7.2) and stored in the dark at 4 °C for further use. Concentrated stock solutions of complexes were prepared by dissolving the complex in DMSO:phosphate buffer (1 : 100) and diluted suitably with phosphate buffer to required concentrations for all the experiments. A 3 ml solution containing appropriate concentration of lysozyme (1 × 10⁻⁶ M) was titrated by successive additions of a 10 μl stock solution of complexes (1 × 10⁻⁵ M). Titrations were manually done by using micropipette for the addition of complexes. For synchronous fluorescence spectra also the same concentration of lysozyme and complexes were used and

Table 1 Experimental data for crystallographic analyses

	1	2	3	4
CCDC deposit number	763002	763001	772056	772085
Formula	C ₁₁ H _{13.8} C ₁₂ CuN ₄ O _{2.9} S	C ₁₂ H ₁₅ Cl ₂ CuN ₄ O _{2.5} S	C ₁₄ H ₁₈ C ₁₂ CuN ₄ O ₂ S	C ₁₈ H ₁₇ ClCuN ₄ O ₂ S
Formula weight	414.96	421.78	440.82	452.41
T/K	110(2)	110(2)	110(2)	110(2)
λ/Å	1.54178	0.71073	0.71073	0.71073
Crystal system	Monoclinic	Monoclinic	Monoclinic	Monoclinic
Space group	P2 ₁ /n	P2 ₁ /n	P2 ₁ /c	P2 ₁ /c
cell dimensions				
a/Å	12.4870(5)	11.042(5)	7.392(6)	8.447(3)
b/Å	10.0729(4)	10.058(5)	24.362(19)	16.895(6)
c/Å	12.6494(5)	15.258(7)	9.914(8)	13.235(5)
α (°)	90	90	90	90
β (°)	101.1650(10)	107.627(6)	102.872(10)	100.997(4)
γ (°)	90	90	90	90
Volume (Å ³)	1560.93(11)	1615.0(13)	1740(2)	1854.1(11)
Z	4	4	4	4
D _c (Mg m ⁻³)	1.766	1.735	1.682	1.621
μ/mm ⁻¹	6.532	1.827	1.697	1.456
F(000)	840	856	900	924
Crystal size (mm ³)	0.12 × 0.10 × 0.07	0.35 × 0.23 × 0.10	0.37 × 0.10 × 0.08	0.60 × 0.36 × 0.34
Independent reflections	2340 [R(int) = 0.0311]	8778 [R(int) = 0.0000]	3980 [R(int) = 0.0572]	4190 [R(int) = 0.0346]
Absorption correction	Semi-empirical from equivalents	Semi-empirical from equivalents	Semi-empirical from equivalents	Semi-empirical from equivalents
Max. and min. transmission	0.6577 and 0.5078	0.8384 and 0.5673	0.8762 and 0.5725	0.6373 and 0.4753
Data/restraints/parameters	2340/0/200	8778/0/210	3980/0/217	4190/0/244
Goodness-of-fit on F ²	1.060	1.037	1.021	1.039
Final R indices [I > 2σ(I)]	R ₁ = 0.0268, wR ₂ = 0.0683	R ₁ = 0.0485, wR ₂ = 0.1277	R ₁ = 0.0334, wR ₂ = 0.0799	R ₁ = 0.0243, wR ₂ = 0.0619
R indices (all data)	R ₁ = 0.0293, wR ₂ = 0.0694	R ₁ = 0.0628, wR ₂ = 0.1368	R ₁ = 0.0472, wR ₂ = 0.0853	R ₁ = 0.0267, wR ₂ = 0.0632
Largest diff. peak & hole/e Å ⁻³	0.745 and -0.312	0.546 and -0.516	0.434 and -0.421	0.358 and -0.396

the spectra were measured at two different $\Delta\lambda$ (difference between the excitation and emission wavelengths of lysozyme) values such as 15 and 60 nm.

Antioxidant assays

The DPPH (2,2'-diphenyl-1-picrylhydrazyl) radical scavenging activity of the complexes was measured according to the method of Blios.⁴⁰ The DPPH radical is a stable free radical having λ_{max} at 517 nm. A fixed concentration of the experimental complex was added to solution of DPPH in methanol (125 μM , 2 ml) and the final volume was made up to 4 ml with double distilled water. The solution was incubated at 37 °C for 30 min in dark. The decrease in absorbance of DPPH was measured at 517 nm.

Total antioxidant activity assay using ABTS cation radical was calculated using the following procedure. ABTS (2,2'-Azino-3-ethylbenzthiazoline-6-sulfonic acid diammonium salt) was dissolved in water to a 5 mM concentration and its cation radical was produced by reacting with 5 mM potassium persulfate. The resulting mixture was kept in dark at room temperature for 12–16 h before use. Prior to assay, the solution was diluted in ethanol (about 1 : 79 v/v) and equilibrated to 30 °C to give an absorbance of 0.70 ± 0.02 at 734 nm. After the addition of 2 ml of diluted ABTS cation radical solution to a fixed concentration of the complex, the absorbance was taken at 30 °C exactly 30 min after the initial mixing.⁴¹

The hydroxyl (OH) radical scavenging activities of the complexes have been investigated using the Nash method.⁴² *In vitro* hydroxyl radicals were generated by Fe³⁺/ascorbic acid system. The detection of hydroxyl radicals was carried out by measuring the amount of formaldehyde formed from the oxidation reaction

with DMSO. The formaldehyde produced was detected spectrophotometrically at 412 nm. A mixture of 1.0 ml of iron-EDTA solution (0.13% ferrous ammonium sulfate and 0.26% EDTA), 0.5 ml of EDTA solution (0.018%), and 1.0 ml of DMSO (0.85% DMSO (v/v) in 0.1 M phosphate buffer, pH 7.4) were sequentially added in the test tubes. The reaction was initiated by adding 0.5 ml of ascorbic acid (0.22%) and incubated at 80–90 °C for 15 min in a water bath. After incubation, the reaction was terminated by the addition of 1.0 ml of ice-cold TCA (17.5% w/v). Subsequently, 3.0 ml of Nash reagent was added to each tube and left at room temperature for 15 min. The intensity of the colour formed was measured spectrophotometrically at 412 nm against reagent blank.

Assay of nitric oxide (NO) scavenging activity was based on the method,⁴³ where sodium nitroprusside in aqueous solution at physiological pH spontaneously generates nitric oxide, which interacted with oxygen to produce nitrite ions that can be estimated using Griess reagent. Scavengers of nitric oxide compete with oxygen leading to reduced production of nitrite ions. For the experiment, sodium nitroprusside (10 mM) in phosphate buffered saline was mixed with a fixed concentration of the complex and incubated at room temperature for 150 min. After the incubation period, 0.5 ml of Griess reagent containing 1% sulfanilamide, 2% H₃PO₄ and 0.1% N-(1-naphthyl) ethylenediamine dihydrochloride was added. The absorbance of the chromophore formed was measured at 546 nm.

The superoxide (O₂⁻) radical scavenging assay was based on the capacity of the complexes to inhibit formazan formation by scavenging the superoxide radicals generated in riboflavin-light-NBT system.⁴⁴ Each 3 ml reaction mixture contained 50 mM sodium phosphate buffer (pH 7.6), 20 μg riboflavin, 12 mM EDTA, 0.1 mg NBT and 1 ml complex solution (20–100 $\mu\text{g ml}^{-1}$).

Reaction was started by illuminating the reaction mixture with different concentrations of complex for 90 s. Immediately after illumination, the absorbance was measured at 590 nm. The entire reaction assembly was enclosed in a box lined with aluminium foil. Identical tubes with reaction mixture kept in dark served as blanks.

For the above five assays, all the tests were run in triplicate and various concentrations of the complexes were used to fix a concentration at which complexes showed in and around 50% of activity. In addition, the percentage of activity was calculated using the formula, % of activity = $[(A_0 - A_c)/A_0] \times 100$. A_0 and A_c are the absorbance in the absence and presence of the tested complex respectively. The 50% of activity (IC_{50}) can be calculated using the percentage of activity results.

Cytotoxicity studies

Cytotoxicity studies were carried out on human cervical cancer cell line (HeLa) and NIH 3T3 mouse embryonic fibroblasts which were obtained from National Centre for Cell Science (NCCS), Pune, India. Cell viability was carried out using the MTT assay method.⁴⁵ The HeLa cells were grown in Eagles minimum essential medium containing 10% fetal bovine serum (FBS) and NIH 3T3 fibroblasts were grown in Dulbeccos modified Eagles medium (DMEM) containing with 10% FBS. For screening experiment, the cells were seeded into 96-well plates in 100 μ l of respective medium containing 10% FBS, at plating density of 10,000 cells/well and incubated at 37 °C, 5% CO₂, 95% air and 100% relative humidity for 24 h prior to addition of complexes. The complexes were dissolved in DMSO and diluted in respective medium containing 1% FBS. After 24 h, the medium was replaced with respective medium with 1% FBS containing the complexes at various concentration and incubated at 37 °C, 5% CO₂, 95% air and 100% relative humidity for 48 h. Triplicate was maintained and the medium containing without the complexes were served as control. After 48 h, 10 μ l of MTT (5 mg ml⁻¹) in phosphate buffered saline

(PBS) was added to each well and incubated at 37 °C for 4h. The medium with MTT was then flicked off and the formed formazan crystals were dissolved in 100 μ l of DMSO and then measured the absorbance at 570 nm using micro plate reader. The % of cell inhibition was determined using the following formula and chart was plotted between % of cell inhibition and concentration and from this IC_{50} value was calculated. % inhibition = $[\text{mean OD of untreated cells (control)}/\text{mean OD of treated cells (control)}] \times 100$.

Results and Discussion

Crystal structures of the complexes

The ORTEP diagrams of the neutral complexes $[\text{CuCl}_2(\text{H}_2\text{-OQtsc-H})] \cdot 2\text{H}_2\text{O}$ (**1**) and $[\text{CuCl}_2(\text{H}_2\text{-OQtsc-Me})] \cdot 2\text{H}_2\text{O}$ (**2**) are given in Fig. 1 and 2. Five donor atoms in a square pyramidal fashion (4+1) surround the copper ion in both **1** and **2**. The basal plane in both the complexes is made up from the O, N, and S atoms of the ligand in its neutral form and one chloride ion, while the second chloride occupies the apical position. The overall geometry of **1** and **2** are very similar; the copper ion lies at about 0.203 Å above the average basal plane towards the axial Cl1 atom in **1** while about the corresponding distance is 0.199 Å in **2**.

The pyramid is fairly regular and the axial Cu–Cl bond length is longer than that of basal one in both the cases which can be ascribed to Jahn–Teller distortion. The dihedral angle between the mean planes of the five-member chelation ring and the six-member one is 10.65° and 11.24° for **1** and **2** respectively. Since the thiosemicarbazone moieties have both the hydrogen bond donors and the hydrogen bond acceptors, the species provide the possibility of forming hydrogen bonds in the crystal. Indeed the complexes are connected through hydrogen bonds involving N2 and N3 nitrogen atoms, the O20 and O21 oxygen atoms of water molecules, and the chlorine atom Cl2, giving three dimensional lattice for **1** (Figure S1) and **2** (Figure S2).† It is to be noted that

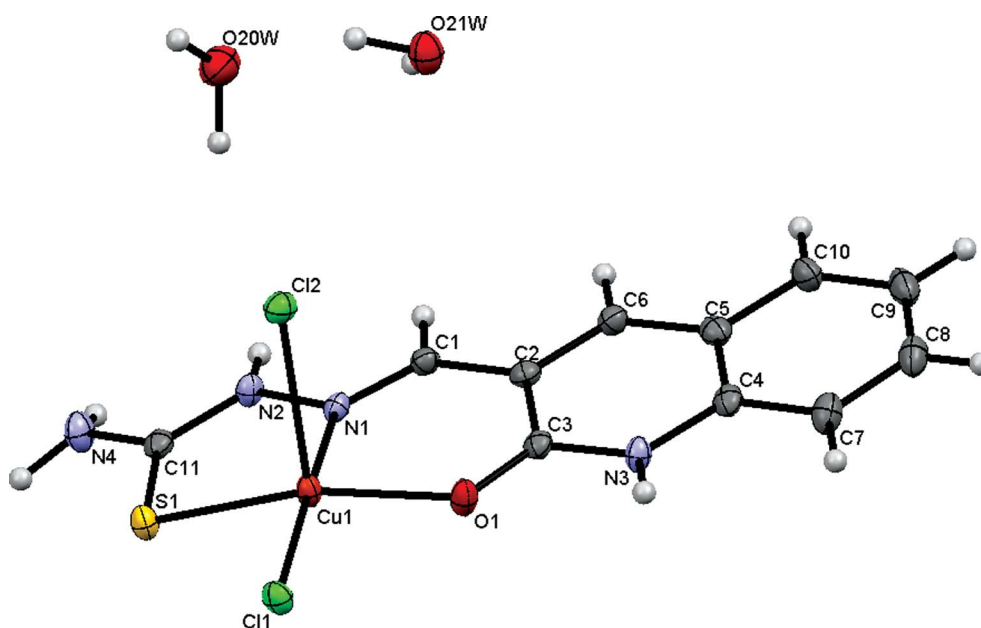


Fig. 1 ORTEP drawing of **1** showing thermal ellipsoids at the 50% probability level.

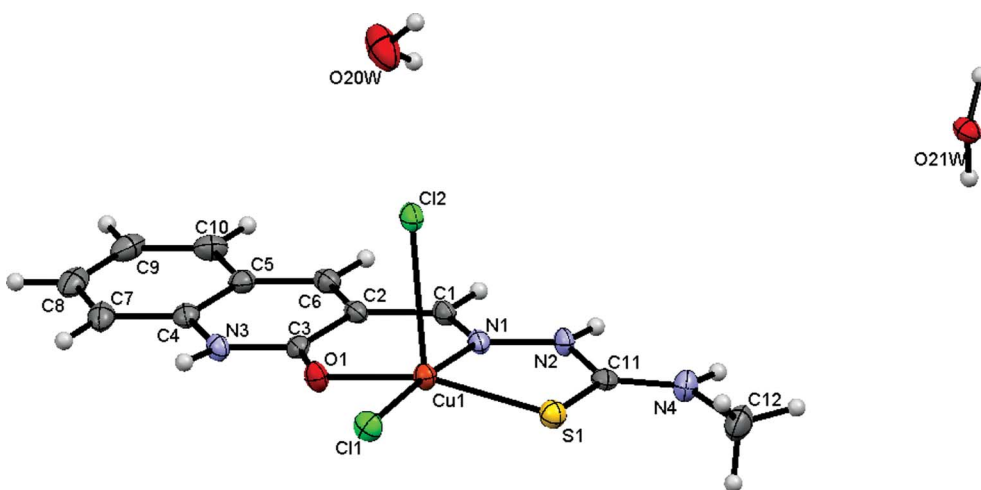


Fig. 2 ORTEP drawing of **2** showing thermal ellipsoids at the 50% probability level.

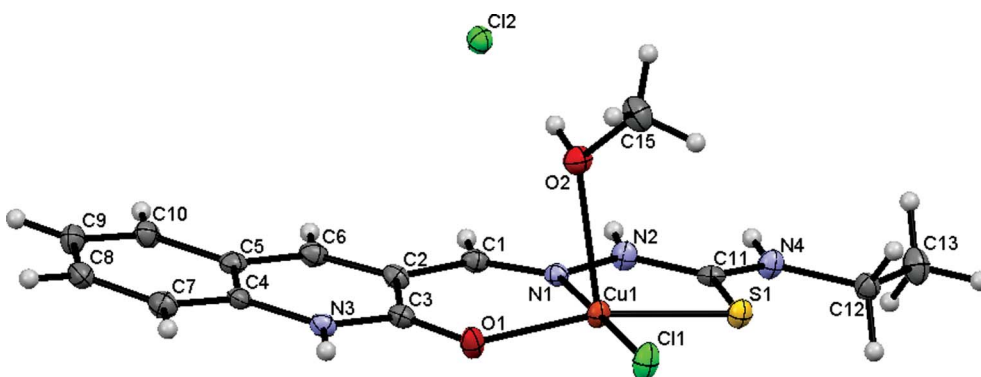


Fig. 3 ORTEP drawing of **3** showing thermal ellipsoids at the 50% probability level.

the chlorine atom Cl1 in **2** has been found involved in the hydrogen bonding but the same has not been seen in **1**.

An ORTEP view of complex **3** is depicted in Fig. 3. The crystal building of **3** is made up of discrete monomeric entities containing five-coordinated copper ion and chloride counter-ions. The geometry of the metal center is close to square pyramid. The quinoline oxygen and azomethine nitrogen atom together with the sulfur that constitutes the thiosemicarbazone ONS chelating set forms the basal plane. The fourth basal position is occupied by one chloride ion. The oxygen from a methanol molecule has taken the apical vertex. Here the copper ion lies at 0.146 Å above the average basal plane towards the apical oxygen of methanol molecule. In addition, there is an appreciable Jahn–Teller effect highlighted by an axial Cu–O2 distance (2.375(2) Å) significantly longer than that observed for Cu–O1 distance (1.9732(18) Å).

The dihedral angle between the mean planes of the five member chelation ring and the six member one is 7.37°. An analysis of the molecular packing suggested that the stabilization of the lattice by several hydrogen bonds, mainly involving the N2, N3, O2 and Cl2. Unlike in **2**, equatorial chlorine atom is not involved in hydrogen bonding in the crystal lattice of **3** (Figure S3).†

An ORTEP view of complex **4** is given in Fig. 4. Complex **4** contains tetra coordinated copper ion with one ONS tridentate uni-negative ligand, one chloride ion and one methanol solvate molecule. The S1–Cu–N1 bond angle (85.45(3)°) is significantly

smaller than that of other three (bond angle of O1–Cu–N1, S1–Cu–Cl1 and O1–Cu–Cl1 is 92.25(4), 93.14(2) and 89.30(3)° respectively) indicating a slightly distorted square planar geometry around copper(II) ion in the complex.

Unlike in **1**, **2** & **3**, sulfur atom is coordinated as negative donor (thiolate and not thione form) in **4**. It may be due to the electron withdrawing nature of phenyl group present in the ligand (H₂-OQtsc-Ph). The Cu1–S1 (2.2436(7) Å) and C11–S1 (1.7483(15) Å) bond lengths very well support this. A very short distance (0.029 Å) between copper ion and the average basal plane and a small dihedral angle (3.07°) between the mean planes of the five member chelation ring and the six member one ensures that the planarity of square should be appreciable.

The molecular packing suggested that the stabilization of the lattice must have been due to several hydrogen bonds, mainly involving the N3, O20 and Cl1 atoms (Figure S4).† The presence of phenyl substitution in aminic nitrogen and the thiolate form of coordinated sulfur provided the conjugation from quinoline ring to terminal N-phenyl ring in **4**. Thus, the above observation clearly reveal that the aliphatic mono substitutions on terminal nitrogen of the thiosemicarbazide chain do not affect the coordination mode of the thiosemicarbazone and the overall geometry of their corresponding copper(II) complexes. But, the phenyl substitution on terminal nitrogen of the thiosemicarbazide chain does affect not only the coordination mode of the thiosemicarbazone but also

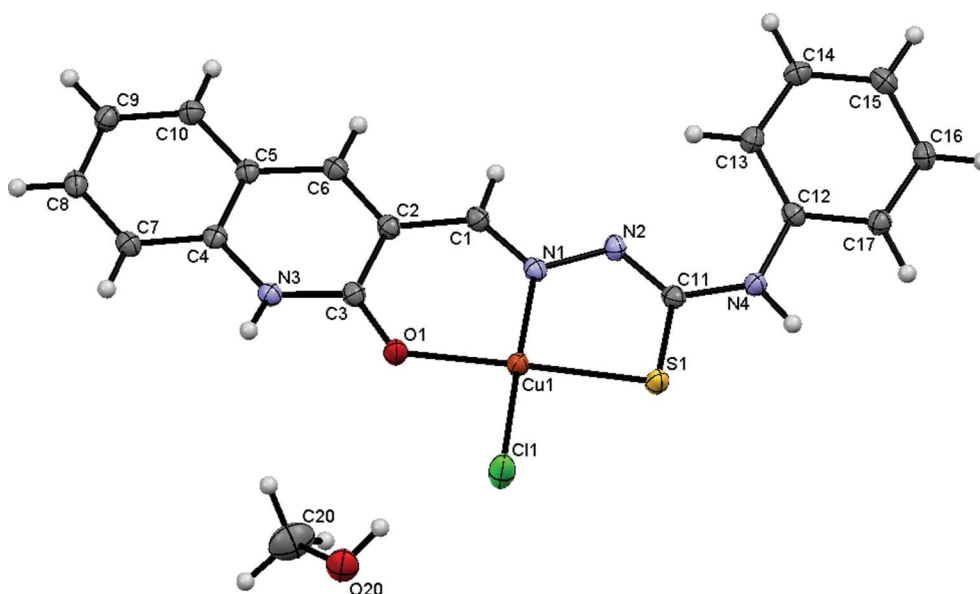


Fig. 4 ORTEP drawing of **4** showing thermal ellipsoids at the 50% probability level.

Table 2 Selected bond distances (Å) and angles (°)

	1	2	3	4
Cu(1)–O(1)	1.9701(16)	1.9726(18)	1.9732(18)	1.9636(11)
Cu(1)–N(1)	1.992(2)	1.991(2)	2.006(2)	1.9704(13)
Cu(1)–Cl(1)	2.2589(7)	2.2515(10)	2.2249(13)	2.2458(8)
Cu(1)–S(1)	2.2618(7)	2.2628(10)	2.2687(13)	2.2436(7)
Cu(1)–Cl(2)	2.6832(7)	2.6897(14)		
Cu(1)–O(2)			2.375(2)	
S(1)–C(11)	1.704(3)	1.703(3)	1.706(2)	1.7483(15)
O(1)–C(3)	1.260(3)	1.261(3)	1.257(3)	1.2622(17)
N(1)–C(1)	1.287(3)	1.294(3)	1.290(3)	1.2952(18)
N(1)–N(2)	1.381(3)	1.375(3)	1.382(3)	1.3913(16)
N(2)–C(11)	1.339(3)	1.357(3)	1.354(3)	1.3078(18)
O(1)–Cu(1)–N(1)	90.03(7)	90.01(8)	89.77(8)	92.25(5)
O(1)–Cu(1)–Cl(1)	90.10(5)	91.31(6)	90.61(7)	174.59(3)
N(1)–Cu(1)–Cl(1)	175.13(6)	175.39(6)	178.17(6)	85.45(4)
O(1)–Cu(1)–S(1)	162.33(6)	162.10(5)	165.33(5)	89.30(3)
N(1)–Cu(1)–S(1)	85.96(6)	86.11(7)	86.17(8)	177.73(3)
Cl(1)–Cu(1)–S(1)	92.47(2)	91.29(4)	93.03(6)	93.14(2)
O(1)–Cu(1)–Cl(2)	94.30(5)	92.96(5)		
N(1)–Cu(1)–Cl(2)	90.21(6)	89.50(6)		
Cl(2)–Cu(1)–Cl(1)	94.63(2)	94.84(3)		
S(1)–Cu(1)–Cl(2)	102.90(2)	104.46(2)		
O(1)–Cu(1)–O(2)			91.36(8)	
N(1)–Cu(1)–O(2)			85.15(8)	
S(1)–Cu(1)–O(2)			102.31(6)	
Cl(1)–Cu(1)–O(2)			96.63(6)	

the overall geometry of its copper(II) complex. The selected bond distances and bond angles of all the complexes are given in Table 2 and they agree very well with those that are reported in other related copper(II) complexes.^{27,46,47}

Protein binding studies

Fluorescence quenching studies. Fluorescence quenching is the decrease in intensity of the fluorescence from a fluorophore that occurs by various types of molecular interactions such as ground state complex formation, excited reactions, energy transfer and collision quenching. Fluorescence quenching measurements have

been widely used to study the interaction of complexes with proteins.^{48–50} Changes in molecular environment in the vicinity of fluorophore can be accessed by the changes in fluorescence spectra in the absence and presence of the complexes and hence provide clues to the nature of the binding phenomenon. The interaction of lysozyme with all the complexes was studied by fluorescence measurement at room temperature (Fig. 5, S5–S7†). A solution of lysozyme (1×10^{-6} M) was titrated with various concentrations of complexes ($0–5 \times 10^{-5}$ M). Fluorescence spectra were recorded in the range of 290–550 nm upon excitation at 280 nm.

The effect of complex **4** on the fluorescence emission spectrum of lysozyme is shown in Fig. 5. Addition of complex **4** to the solution of lysozyme resulted in the decrease of its fluorescence intensity accompanied by a small blue shift. The observed blue shift is mainly due to the fact that the active site in protein is buried in a hydrophobic environment which suggests the interaction of complex **4** with the drug carrier protein.

The fluorescence quenching can be described by Stern–Volmer relation:

$$I_0/I = 1 + K_{SV}[Q] \quad (1)$$

where I_0 and I are the fluorescence intensities of the fluorophore in the absence and presence of quencher, K_{SV} is the Stern–Volmer quenching constant and $[Q]$ is the quencher concentration. The K_{SV} value is obtained as a slope from the plot of I_0/I vs. $[Q]$.

The fluorescence quenching mechanisms are usually classified as either static or dynamic quenching. A simple method to explore the type quenching is UV-Visible absorption spectroscopy. Fig. 6 shows the absorption spectrum of lysozyme, complex **4** and lysozyme-complex**4**.

In the presence of complex **4**, the absorbance of lysozyme increases and a slight red shift was observed. This indicates that the interaction between lysozyme and complex **4** is a static one and it was involved in the formation of ground state complex of the type lysozyme...complex **4**. But, dynamic quenching affects only the excited state while it has no function on the absorption spectrum.

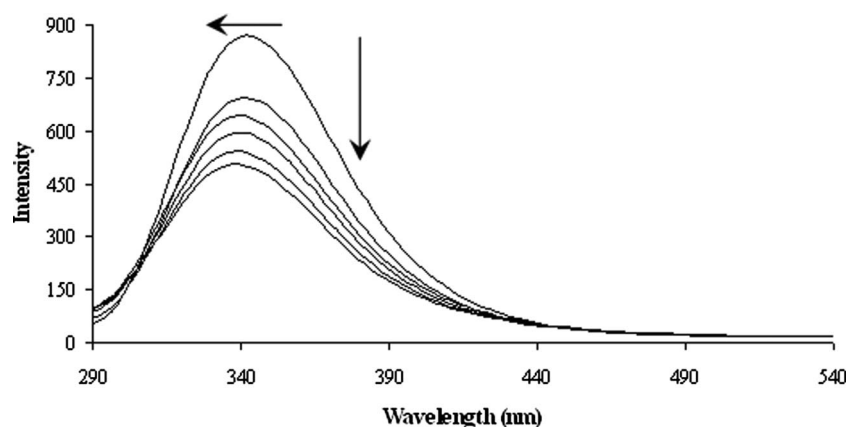


Fig. 5 The emission spectrum of lysozyme (1×10^{-6} M; $\lambda_{\text{exc}} = 280$ nm; $\lambda_{\text{emi}} = 347$ nm) in the presence of increasing amounts of complex **4** (0, 1, 2, 3, 4 and 5×10^{-5} M). Arrows show the fluorescence quenching accompanied by blue shift upon increasing concentration of complex **4**.

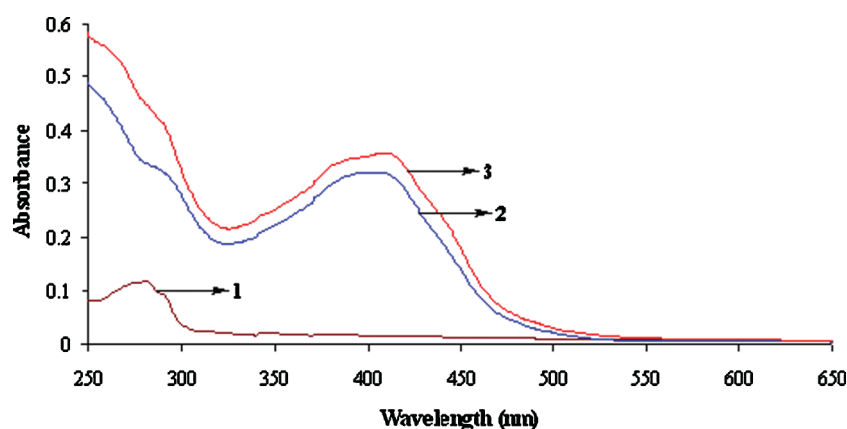


Fig. 6 Absorption spectra of (1) lysozyme (1×10^{-6} M), (2) complex **4** (1×10^{-5} M) and (3) lysozyme-complex **4** [lysozyme = 1×10^{-6} M and complex **4** = 1×10^{-5} M].

Therefore, the mechanism is only static quenching. The absorption spectra of lysozyme-complex **1** (Figure S8), lysozyme-complex **2** (Figure S9) and lysozyme-complex **3** (Figure S10) also have the same phenomena.† Similar type of static interaction between protein with drug molecule has been previously reported.⁵¹

If it is assumed that the binding of proteins to complex occurs at equilibrium, the equilibrium binding constant and the number of binding sites can be analyzed according to the Scatchard equation:

$$\log \left[\frac{F_0 - F}{F} \right] = \log K + n \log [Q] \quad (2)$$

where K is the binding constant of quencher with lysozyme, n is the number of binding sites, F_0 and F are the fluorescence intensity in the absence and presence of the quencher. The value of K can be determined from the slope of $\log [(F_0 - F)/F]$ versus $\log [Q]$ as shown in Fig. 7.

The calculated value of binding constant (K) and the number of binding sites (n) are listed in Table 3. The binding constant values indicate that the complexes bind to lysozyme in the series of complex **4** > complex **3** > complex **2** > complex **1**. The observed blue shift can be correlated with the binding of the complexes with protein that makes it more hydrophobic environment. Complex **1** possesses a free amino group while the other complexes **2**, **3**, **4** have methyl, ethyl, phenyl substitutions. Complex **4** possesses a

Table 3 Binding constant and number of binding sites for the interactions of complexes with lysozyme

System	K (M)	n	$^a R^2$
Lysozyme + Complex 1	9.2×10^3	0.7675	0.9952
Lysozyme + Complex 2	1.1×10^4	0.9615	0.9828
Lysozyme + Complex 3	7.6×10^4	1.1726	0.9913
Lysozyme + Complex 4	2.1×10^6	1.5643	0.9934

^a R^2 is the correlation coefficient.

phenyl group, which can interact with the active site by making it more hydrophobic. On decreasing the bulkiness in substitution, the binding constant value (K) also decreases. The larger value of K indicates a strong interaction between the lysozyme and the complexes.

Characteristics of synchronous fluorescence spectra

Synchronous fluorescence spectra provide information on the molecular micro-environment, particularly in the vicinity of the fluorophore functional groups.⁵² The fluorescence of lysozyme is due to presence of tyrosine and tryptophan residues. Among them, tryptophan is the most dominant fluorophore, located at the substrate binding sites. Most of the drugs bind to the

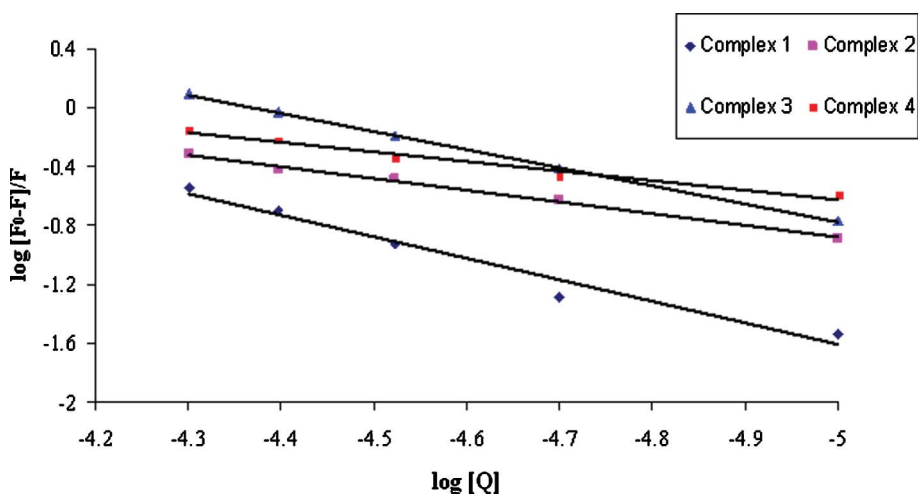


Fig. 7 Plot of $\log [(F_0 - F)/F]$ vs. $\log [Q]$.

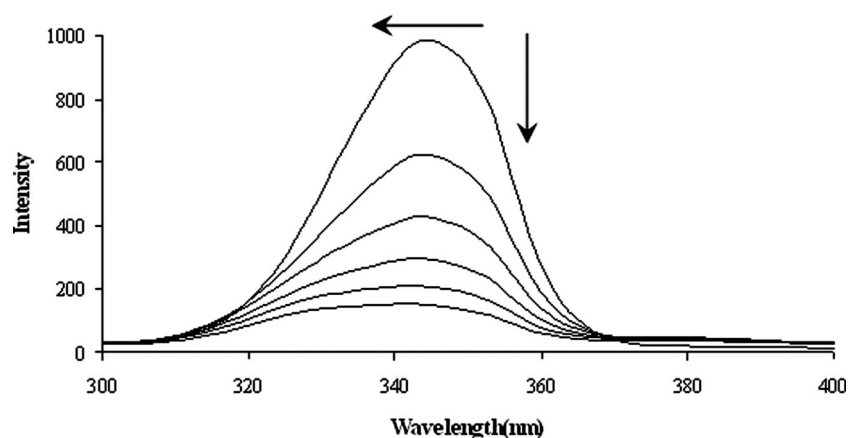


Fig. 8 Synchronous spectra of lysozyme (1×10^{-6} M) in the presence of increasing amounts of complex 4 ($0, 1, 2, 3, 4$ and 5×10^{-5} M) in the wavelength difference of $\Delta\lambda = 60$ nm. Arrows show the emission intensity decrease accompanied by blue shift upon the increasing concentration of complex 4.

protein in the active binding sites. Hence, synchronous method is usually applied to find out the conformational changes around tryptophan and tyrosine region. In synchronous fluorescence spectroscopy, according to Miller,⁵³ the difference between the excitation wavelength and emission wavelength ($\Delta\lambda = \lambda_{\text{emi}} - \lambda_{\text{exc}}$) indicates the type of chromophores. A higher $\Delta\lambda$ value such as 60 nm is indicative of the characteristic of tryptophan residue while a lower λ value such as 15 nm is characteristic of tyrosine residue.⁵⁴ The synchronous fluorescence spectra of lysozyme with various concentrations of **1**, **2**, **3** and **4** were recorded at $\Delta\lambda = 15$ nm (Figures S11–S14) and $\Delta\lambda = 60$ nm (Fig. 8, S15–S17†), respectively. The fluorescence intensities of both the tryptophan and tyrosine were decreased but the emission wavelength of the tryptophan residues is blue shifted with increasing concentration of complex **4**. At the same time, there is no change in the emission wavelength of tyrosine. It suggests that the interaction of complex **4** with lysozyme affects the conformation of tryptophan micro-region. The other complexes also show a blue shift in tryptophan region (Figures S15–S17†). It reveals that the hydrophobicity around tryptophan residues is strengthened. The hydrophobicity observed in fluorescence and synchronous measurements confirmed the effective binding of all the complexes with the lysozyme. Hence,

the strong interaction of these complexes with lysozyme suggests that the complexes may be fit for anticancer studies.

Antioxidant activity

In the antioxidant activity of all the complexes evaluated in a series of *in vitro* assay involving hydroxyl radicals, DPPH radicals, ABTS cation radicals, nitric oxide and superoxide anion radicals, the IC_{50} values have been determined. The IC_{50} value of all complexes (Chart 1) obtained from different type of assay experiments strongly supports that all the complexes possess excellent antioxidant activities, which are much better than that of standard antioxidants like mannitol and vitamin C.⁵⁵ The copper metal chelation gives almost a planar structure for all the complexes which is responsible for their antioxidant activity.

In general, the Cu(II) complexes showed antioxidant activity in the order of $4 > 3 > 2 > 1$ in all the experiments. The ABTS cation radical scavenging power of the tested complexes was the most and NO scavenging was the least. **1** and **2** having similar structure showed almost comparable antioxidant activities. But, **3** showed better radical scavenging activities over **1** and **2** which may be due to the fact that it has one coordinated methanol

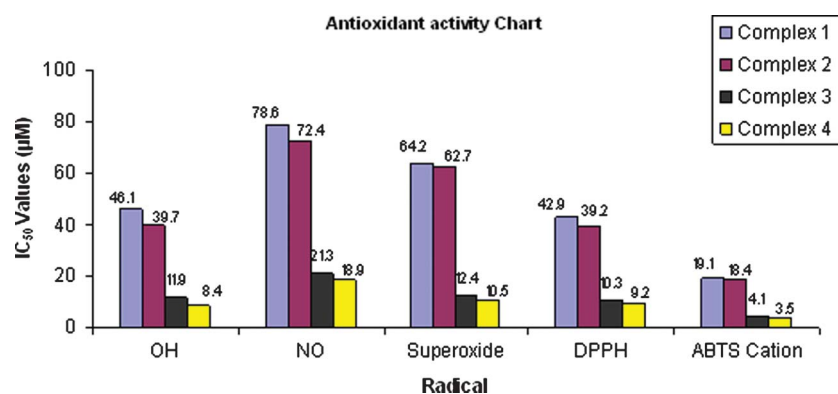


Chart 1 Antioxidant activity of the complexes.

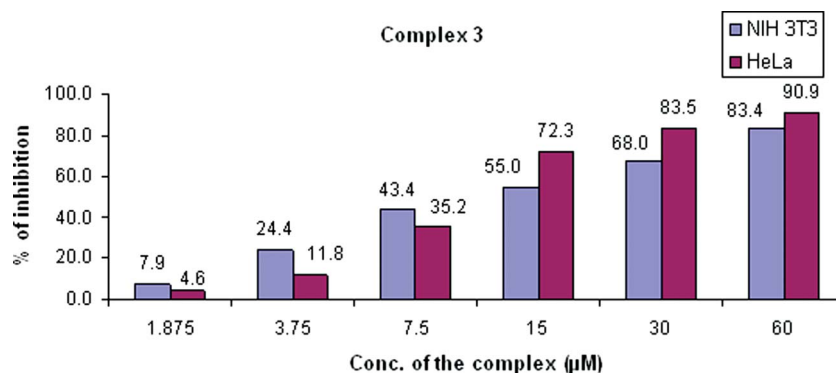


Chart 2 The % of inhibition at various conc. of 3 on NIH3T3 and HeLa cell line.

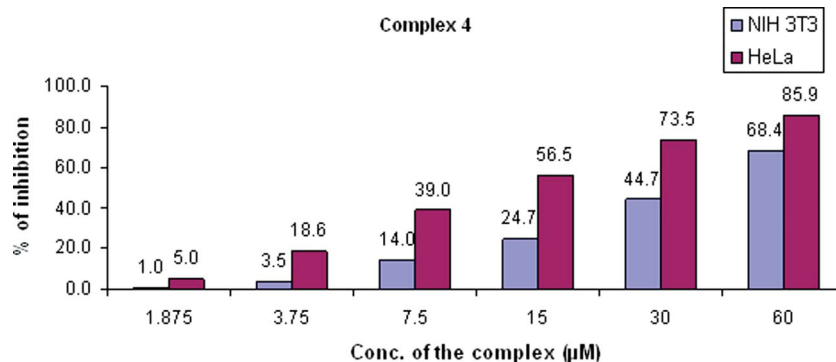


Chart 3 The % of inhibition at various conc. of 4 on NIH3T3 and HeLa cell line.

molecule in it. However, **4** showed the highest activity among all the complexes which may be due to the phenyl substitution in the terminal nitrogen of the ligand and to the square planar geometry of the complex.

Study of cytotoxicity by MTT Assay

MTT assay was performed on HeLa (human cervical cancer cell line) to check the anticancer activity and on NIH 3T3 (normal mouse embryonic fibroblasts cell line) to study the toxicity of complexes **1–4**. Complex **1** and **2** did not show any significant activity even up to 1000 µM of complexes on both the cells. However, complexes **3** and **4** showed excellent activity on both the cells. When the concentration of complexes **3** and **4** were increased from 1.875 µM to 60 µM, an increase in the percentage of cell

inhibition was observed with both the complexes on both the cells. An inhibition of 83.4% NIH 3T3 cell and 90.9% in HeLa were observed with 60 µM of complex **3** (Chart 2). Cell inhibition of 68.5% in NIH 3T3 and 85.9% in HeLa were observed with 60 µM of complex **4** (Chart 3).

From the IC₅₀ values (Chart 4), complex **4** showed low toxicity against normal NIH 3T3 cell and high cytotoxicity against HeLa cancer cell over complex **3**. It may be due to the square planar geometry of complex **4**. But, complexes **1** and **2** showed very low activity because both these complexes are square pyramidal and have low planarity which may influence the cytotoxic activity. However, the complex **3** showed better activity though it has square pyramidal geometry which may be due to the presence of coordinated methanol and cationic nature of the complex. The substitution of a phenyl group at terminal nitrogen of

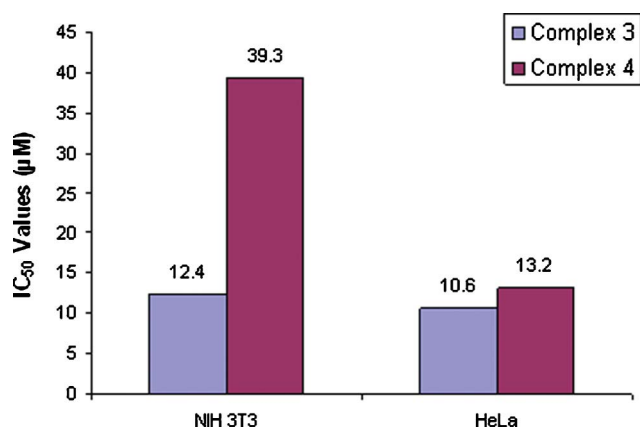


Chart 4 The IC₅₀ value (in µM) of **3** and **4** on NIH3T3 and HeLa cell line.

the coordinated ligand and the planarity of complex **4** may be responsible for its observed excellent cytotoxic activity over the other three complexes. The observed potency, selectivity and low toxicity of the complex **4** suggest the need for synthesizing some more compounds of this type for better activity. Hence, a detailed study on the structure-activity of the complexes and mechanisms of their biological activities needs to be done.

Conclusion

A series of copper(II) complexes containing 2-oxo-1,2-dihydroquinoline-3-carbaldehyde N-substituted thiosemicarbazone has been prepared and characterized in order to study the effect of substitution at terminal N of the ligand on the structures of the complexes formed and their biological activities. The presence of phenyl group in terminal nitrogen has in fact altered the coordination mode of thiosemicarbazone from ONS to ONS⁻ and also the geometry of the complexes from square pyramidal to square planar. The protein binding properties of the complexes examined by the fluorescence spectra suggested that the binding affinity increases with the increase in size of substitution at terminal nitrogen of the thiosemicarbazone moiety. The results from various radical scavenging assay showed that the methanol coordination and cationic nature of the complex increases the activity of square pyramidal complexes though it was slightly less compared to that of square planar complex. The cytotoxic studies showed that the complexes **3** and **4** exhibit good cytotoxic activity against HeLa and NIH 3T3 cell lines. The IC₅₀ cytotoxicity values indicated that the complex **4** is less toxic but more cytotoxic over complex **3**. All encouraging chemical and biological findings indicate that these complexes are very promising candidates as live-cell imaging reagents that could contribute to the understanding of cellular uptake of metal complexes. Further studies are needed to assess their pharmacological properties *in vivo* and to elucidate the actual mechanism of their biological activity.

Acknowledgements

Financial assistance received from the Council of Scientific and Industrial Research, New Delhi, India [Grant No. 01(2216)/08/EMR-II & 21(0745)/09/EMR-II], is gratefully acknowledged.

References

- 1 I. Papanastasiou, A. Tsoinis, N. Kolocouris, S. R. Prathalingam and J. M. Kelly, *J. Med. Chem.*, 2008, **51**, 1496–1500.
- 2 D. Sriram, P. Yogeewari, R. Thirumurugan and R. K. Pavana, *J. Med. Chem.*, 2006, **49**, 3448–3450.
- 3 J. P. Scovill, D. L. Klayman and D. G. Franchino, *J. Med. Chem.*, 1982, **25**, 1261–1264.
- 4 H. Huang, Q. Chen, X. Ku, L. Meng, L. Lin, X. Wang, C. Zhu, Y. Wang, Z. Chen, M. Li, H. Jiang, K. Chen, J. Ding and H. Liu, *J. Med. Chem.*, 2010, **53**, 3048–3064.
- 5 N. Farrell, *Coord. Chem. Rev.*, 2002, **232**, 1–4.
- 6 J. Peisach and P. Aisen, *The Biochemistry of Copper*, ed. W. Blumberg, Academic Press, New York, 1966.
- 7 E. I. Solomon, R. K. Szilagyi, S. D. George and L. Basumallick, *Chem. Rev.*, 2004, **104**, 419–458.
- 8 T. Wang and Z. Guo, *Curr. Med. Chem.*, 2006, **13**, 525–537.
- 9 I. H. Hall, C. B. Lackey, T. D. Kistler, R. W. Durham, E. M. Jouad, M. Khan, X. D. Thanh, S. Djebbar-Sid, O. Benali-Baitich and G. M. Bouet, *Pharmazie*, 2000, **55**, 937–941.
- 10 Q. L. Yue, Z. H. Song and F. X. Dong, *Spectrochim. Acta, Part A*, 2008, **69**, 1097–1102.
- 11 H. Liang, J. Huang, C. Q. Tu, M. Zhang, Y. Q. Zhou and P. W. Shen, *J. Inorg. Biochem.*, 2001, **85**, 167–171.
- 12 H. Liang, X. C. Shen, Z. L. Jiang, X. W. He and P. W. Shen, *Sci. China, Ser. B: Chem.*, 2000, **43**, 600–608.
- 13 Y. Q. Wang, H. M. Zhang, G. C. Zhang, W. H. Tao, Z. H. Fei and Z. T. Liu, *J. Pharm. Biomed. Anal.*, 2007, **43**, 1869–1875.
- 14 Y. P. Wang, Y. L. Wei and C. Dong, *J. Photochem. Photobiol., A*, 2006, **177**, 6–11.
- 15 Y. J. Hu, Y. Liu, R. M. Zhao, J. X. Dong and S. S. Qu, *J. Photochem. Photobiol., A*, 2006, **179**, 324–329.
- 16 J. H. Tang, F. Luan and X. G. Chen, *Bioorg. Med. Chem.*, 2006, **14**, 3210–3217.
- 17 C. Dufour and O. Dangles, *Biochim. Biophys. Acta, Gen. Subj.*, 2005, **1721**, 164–173.
- 18 H. F. Ji and H. Y. Zhang, *Chem. Res. Toxicol.*, 2004, **17**, 471–475.
- 19 E. Pontiki, D. Hadjipavlou-Litina, A. T. Chaviara and C. A. Bolos, *Bioorg. Med. Chem. Lett.*, 2006, **16**, 2234–2237.
- 20 P. Nordell and P. Lincoln, *J. Am. Chem. Soc.*, 2005, **127**, 9670–9671.
- 21 P. Barraja, P. Diana, A. Montalbano, G. Dattolo, G. Cirrincione, G. Viola, D. Vedaldi and F. D. Acqua, *Bioorg. Med. Chem.*, 2006, **14**, 8712–8728.
- 22 J. T. Kuethe, A. Wong, C. X. Qu, J. Smithrovich, I. W. Davies and D. L. Hughes, *J. Org. Chem.*, 2005, **70**, 2555–2567.
- 23 J. DeRuiter, A. N. Brubaker, W. L. Whitmer and J. L. Stein, *J. Med. Chem.*, 1986, **29**, 2024–2028.
- 24 P. Hewawasam, W. Fan, J. Knipe, S. L. Moon, C. G. Boissard, V. K. Gribkoff and J. E. Starett, *Bioorg. Med. Chem. Lett.*, 2002, **12**, 1779–1783.
- 25 J. Rousell, E. B. Haddad, J. C. Mak, B. L. Webb, M. A. Giembycz and P. J. Barnes, *Mol. Pharmacol.*, 1996, **49**, 629–635.
- 26 I. V. Ukrainets, V. O. Gorokhova, A. P. Benzuglyi and V. L. Sidorenko, *Farm. Zh.*, 2002, **1**, 75–80.
- 27 Z. C. Liu, B. D. Wang, Z. Y. Yang, Y. Li, D. D. Qin and T. R. Li, *Eur. J. Med. Chem.*, 2009, **44**, 4477–4484.
- 28 A. G. Quiroga and C. N. Ranninger, *Coord. Chem. Rev.*, 2004, **248**, 119–133.
- 29 D. L. Klayman, J. F. Bartosovich, T. S. Griffin, C. J. Mason and J. P. Scovill, *J. Med. Chem.*, 1979, **22**, 855–862.
- 30 D. L. Klayman, J. P. Scovill, J. F. Bartosovich and C. J. Mason, *J. Med. Chem.*, 1979, **22**, 1367–1373.
- 31 D. Kovala-Demertzi, P. N. Yadav, M. A. Demertzis and M. Coluccia, *J. Inorg. Biochem.*, 2000, **78**, 347–354.
- 32 J. P. Scovill, D. L. Klayman and C. F. Franchino, *J. Med. Chem.*, 1982, **25**, 1261–1264.
- 33 U. Abram, K. Ortner, R. Gust and K. Sommer, *J. Chem. Soc., Dalton Trans.*, 2000, 735–744.
- 34 T. S. Lobana, R. Sharma, G. Bawa and S. Khanna, *Coord. Chem. Rev.*, 2009, **253**, 977–1055.
- 35 M. K. Singh, A. Chandra, B. Singh and R. M. Singh, *Tetrahedron Lett.*, 2007, **48**, 5987–5990.
- 36 SAINT (Version 7). “Program for Data Integration from Area Detector Frames”, Bruker-Nonius Inc., 5465 East Cheryl Parkway, Madison, WI 53711-5373 USA.

- 37 APEX2 "Program for Data Collection on Area Detectors" BRUKER AXS Inc., 5465 East Cheryl Parkway, Madison, WI 53711-5373 USA.
- 38 G. M. Sheldrick, "SADABS (version 2008/1): Program for Absorption Correction for Data from Area Detector Frames", University of Göttingen, 2008.
- 39 I. J. Bruno, J. C. Cole, P. R. Edgington, M. K. Kessler, C. F. Macrae, P. McCabe, J. Pearson and R. Taylor, *Acta Crystallogr., Sect. B: Struct. Sci.*, 2002, **58**, 389–397.
- 40 M. S. Blois, *Nature*, 1958, **181**, 1199–1200.
- 41 R. Re, N. Pellegrini, A. Prolegente, A. Pannala, M. Yang and C. Rice-Evans, *Free Radical Biol. Med.*, 1999, **26**, 1231–1237.
- 42 T. Nash, *Biochem. J.*, 1953, **55**, 416–421.
- 43 L. C. Green, D. A. Wagner, J. Glogowski, P. L. Skipper, J. S. Wishnok and S. R. Tannenbaum, *Anal. Biochem.*, 1982, **126**, 131–138.
- 44 C. Beauchamp and I. Fridovich, *Anal. Biochem.*, 1971, **44**, 276–287.
- 45 M. Blagosklonny and W. S. El-diery, *Int. J. Cancer*, 1996, **67**, 386.
- 46 M. Belicchi-Ferrari, G. Gasparri-Fava, E. Leporati, G. Pelosi, R. Rossi, P. Tarasconi, R. Albertini, A. Bonati, P. Lunghi and S. Pinelli, *J. Inorg. Biochem.*, 1998, **70**, 145–154.
- 47 M. Baldini, M. Belicchi-Ferrari, F. Bisceglie, G. Pelosi, S. Pinelli and P. Tarasconi, *Inorg. Chem.*, 2003, **42**, 2049–2055.
- 48 S. M. T. Shaikh, J. Seetharamappa, S. Ashoka and P. B. Kandagal, *Dyes Pigm.*, 2007, **73**, 211–216.
- 49 S. Bi, D. Song, Y. Tian, X. Zhou, Z. Liu and H. Zhang, *Spectrochim. Acta, Part A*, 2005, **61**, 629–636.
- 50 X. Z. Feng, Z. Lin, L. J. Yang, C. Wang and C. Bai, *Talanta*, 1998, **47**, 1223–1229.
- 51 Y. Hu, Y. Yang, C. Dai, Y. Liu and X. Xiao, *Biomacromolecules*, 2010, **11**, 106–112.
- 52 G. Z. Chen, X. Z. Huang, J. G. Xu, Z. B. Wang and Z. Z. Zhang, *Method of Fluorescent Analysis*, 2nd ed., Science Press, Beijing, 1990.
- 53 J. N. Miller, *Proc. Anal. Div. Chem. Soc.*, 1979, **16**, 203–208.
- 54 E. A. Brustein, N. S. Vedenkina and M. N. Irkova, *Photochem. Photobiol.*, 1973, **18**, 263–279.
- 55 N. Yilmaz, H. Dulger, N. Kiymaz, C. Yilmaz, B. O. Gudu and I. Demir, *Brain Res.*, 2007, **1164**, 132–135.